Available online at www.sciencedirect.com
SCIENCE DIRECT
Surface & Coatings Technology 190 (2005) 155–164
SURFACE & COATINGS TECHNOLOGY
www.elsevier.com/locate/surfcoat

Evaluation of WC–17Co and WC–10Co–4Cr thermal spray coatings by HVOF on the fatigue and corrosion strength of AISI 4340 steel

H.J.C. Voorwald[b], R.C. Souza[a], W.L. Pigatin[c], M.O.H. Cioffi[b,d,*]

[a]*FAENQUIL/DEMAR–Department of Materials Engineering, Pólo Urbo-Industrial, Gleba AI-6, CP 116 CEP 12600-000, Lorena/SP, Brazil*
[b]*Fatigue and Aeronautic Material Research Group–Department of Material and Technology, UNESP, Av. Ariberto Pereira da Cunha, 333 CEP 12516-410 Guaratinguetá-SP, Brazil*
[c]*EMBRAER-LIEBHERR Airplanes/Brazil S.A.*
[d]*IPOLI-UNESP/Sorocaba, Av. 3 de março, 511 CEP 18087-180 Sorocaba/SP, Brazil*

Received 9 July 2003; accepted in revised form 9 August 2004
Available online 28 October 2004

Abstract

It is known that chromium electroplating is related to the reduction in the fatigue strength of base metal. However, chromium results in protection against wear and corrosion combined with chemical resistance and good lubricity. Environmental requirements are an important point to be considered in the search for possible alternatives to hard chrome plating. Aircraft landing gear manufactures are considering WC thermal spray coating applied by the high-velocity oxygen-fuel (HVOF) process an alternative candidate, which shows performance at least comparable to results, obtained for hard chrome plating. The aim of this study is to compare the influence of WC–17Co and WC–10Co–4Cr coatings applied by HVOF process and hard chromium electroplating on the fatigue strength of AISI 4340 steel, with and without shot peening. *S–N* curves were obtained in axial fatigue test for base material, chromium plated and tungsten carbide coated specimens. Tungsten carbide thermal spray coating results in higher fatigue strength when compared to hard chromium electroplated. Shot peening prior to thermal spraying showed to be an excellent alternative to increase fatigue strength of AISI 4340 steel. Experimental data showed higher axial fatigue and corrosion resistance in salt fog exposure for samples WC–10Co–4Cr HVOF coated when compared with WC–17Co. Fracture surface analysis by scanning electron microscopy (SEM) indicated the existence of a uniform coverage of nearly all substrates.

Keywords: Fatigue; Corrosion; Thermal spray; AISI 4340 steel

1. Introduction

Coatings deposited onto various substrates are used in a wide range of applications in important industrial sectors including aerospace, automotive, and petrochemical fields. Chromium plating is the most used electroplated coating to obtain high level of hardness, wear and corrosion resistance, and a low coefficient of friction [1,2]. However, the plating bath contains hexavalent chromium that has adverse health and environmental effects. Increasingly stringent regulations are making chromium plating more expensive for manufactures and repair facilities [3,4].

Electroplating has as significant characteristic the high internal residual tensile stress originated from the decomposition of chromium hydrides during electrodeposition process [5–7]. This residual stress increases with thickness growing and is relieved by local microcrackings produced during electroplating. Consequently, microcracks density is related to the high internal tensile residual stress, hardness, and corrosion resistance [2,5,8,9]. Fatigue is an important parameter to be considered in the behavior of mechanical components subjected to constant and variable amplitude loading. Fatigue resistance of a structural component can be influenced by mechanical, metallurgical, and environmental variables [10]. In high-strength steel, surface and subsurface

* Corresponding author. Tel.: +55 12 31232865; fax: +55 12 31232852.
E-mail address: cioffi@sorocaba.unesp.br (M.O.H. Cioffi).

0257-8972/$ - see front matter © 2004 Elsevier B.V. All rights reserved.
doi:10.1016/j.surfcoat.2004.08.181

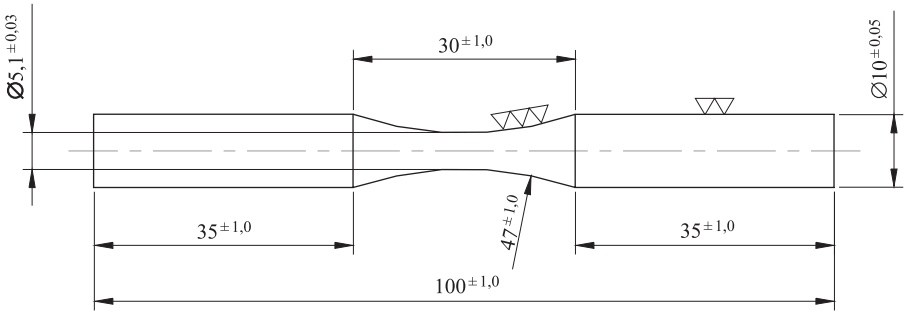

Fig. 1. Axial fatigue testing specimen.

defects play an important role in the reduction of fatigue limit [11].

It is well known that the hard chromium electroplating decreases the fatigue resistance of a component, which is attributed to high residual tensile stress and microcracks density contained into the coating [12]. Failure of the hard chrome plating is frequently governed by initiation and propagation of these microcracks [13,14].

According to Pina et al. [15], these residual stresses achieve values around of 800 MPa tensile at surface. Experimental results in bending fatigue tests on samples with different coatings and coating conditions show that the fatigue strength is dependent on the fracture behavior of the substrates and on the hardness and residual stress at the substrate surface [16].

As a consequence, by the fact that chrome plating can result in fatigue strength lower than those of uncoated parts, the replacement of these surface treatments by thermal spray coatings is considered to be a possible alternative [12]. A promising technique to produce hard and wear resistance coatings that could replace hard chromium electroplating in a number of applications is high-velocity oxygen-fuel (HVOF) thermal spraying. The HVOF process is capable of depositing metal alloy, ceramic/metal composite, polymer coating rapidly and with thickness values comparable to those of hard chrome electroplating [12]. HVOF thermally sprayed WC–Co coatings with excellent wear resistance properties have been widely used in aerospace, oil, and paper industries. Considering their practical applications, fatigue strength of components WC–Co coated is an important parameter to be evaluated.

To improve fatigue resistance, the shot peening process was used in order to induce superficial compressive residual stress in the material which delay the nucleation and propagation of fatigue cracks [17–19]. The shot peening is controlled, in industries, with thin plates, which are placed in parallel to the treated material, called Almen plates. The deflected shaped caused by the process called Almen intensity is appropriated to adjust the shot peening parameters [20,21].

Experiments have shown relaxation of the compressive residual stress field (CRSF) induced by shot peening, over the fatigue life [19,22–26].

High-velocity oxy-fuel thermal spraying has been shown to produce more wear resistant coatings than, for example, those obtained by hard chromium electroplating [27]. Tungsten carbide–cobalt (WC–Co) coatings are used in some cases to replace chromium plating or anodizing, due to

Table 1
Axial fatigue tests

Specimens number	Materials	Process	Thickness (μm)
12	Base material		
12	Base material/Hard chromium	Electroplating	160
12	Base material/WC–17%Co	HP/HVOF I	150
12	Base material/WC–17%Co	HVOF II	150
12	Base material/WC–10Co–4Cr	HP/HVOF I	170
12	Base material/WC–10Co–4Cr	HVOF II	170
12	Base material/WC–10Co–4Cr with shot peening	HP/HVOF I	170
12	Base material/WC–10Co–4Cr With shot peening	HVOF II	170

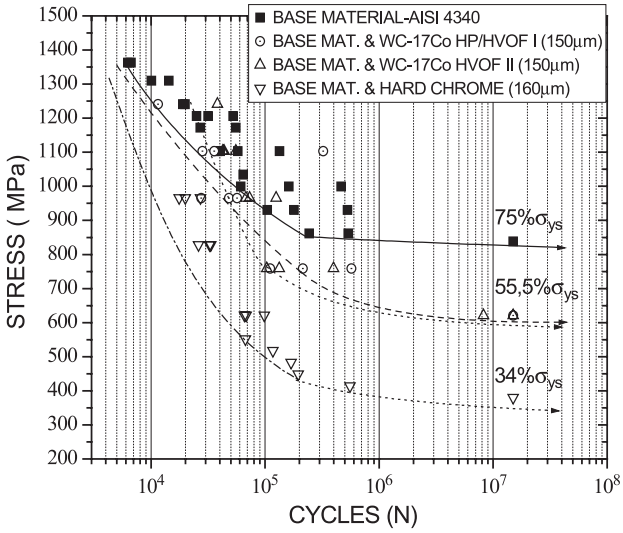

Fig. 2. Axial fatigue $\sigma \times N$ curves. Base material (■); base material coated with WC–17Co by HP/HVOF I process (⊙); base material coated with WC–17Co by HVOF II process (△); and base material electroplated with hard chromium (▽).

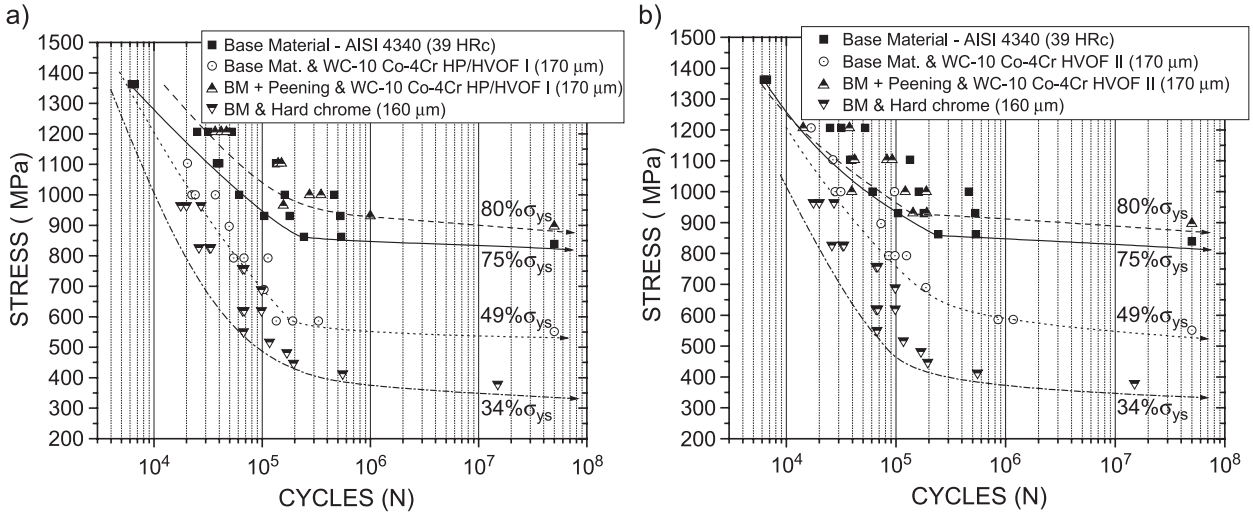

Fig. 3. (a–b) Axial fatigue $\sigma \times N$ curves. Base material; base material coated with WC–10Co–4Cr by HP/HVOF I process; base material coated with WC–10Co–4Cr by HVOF II process; and base material electroplated with hard chromium.

their wear resistant characteristics. Comparison between WC–12Co and WC–17Co coatings indicates higher friction coefficients for the later, as a consequence of the larger amount of metallic matrix present [28].

Protection against corrosion plays an important role in the aerospace industry. Experimental tests conducted to determine corrosion resistance according to ASTM B 117 indicate better protection with electroless nickel interlayer on chromium-plated AISI 4340 steel [9].

Fatigue strength, abrasive wear, and corrosion resistance of AISI 4340 steel chromium-electroplated was compared with WC–17Co and WC–10Co–4Cr coatings applied by high-velocity oxy-fuel (HVOF) process. Scanning electron microscopy technique (SEM) and optical microscopy were used to observe crack origin sites and the existence of a uniform coverage of nearly all substrates, thickness and adhesive in all coatings.

2. Experimental

AISI 4340 steel samples, used in landing gear components where strength and toughness are fundamental design requirements, were tested. Chemical analysis conducted has as results: 0.39% C, <0.001% S, 0.69% Mn, 0.74% Cr, 1.70% Ni, and 0.23% Mo. The fatigue experimental program was performed on axial fatigue test specimens machined from hot-rolled, quenched, and tempered bars according to Fig. 1.

Specimens were polished in the reduced section with 600 grit papers, inspected dimensionally and the magnetic particle inspection. Mechanical properties of AISI 4340 steel used are 39 HRc, yield tensile strength of 1118 MPa, and ultimate tensile strength 1210 MPa. Those properties were obtained by means of quenching from 815–845 °C in oil (20 °C) followed by tempering in the range 520±5 °C for 2 h. At last, samples were subjected

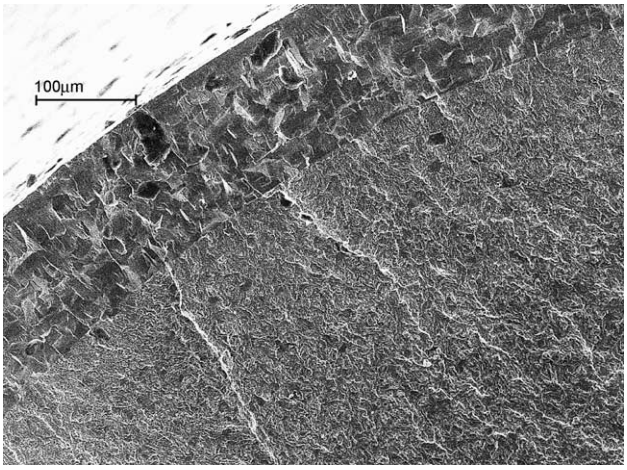

Fig. 4. Fracture surface from specimen hard chromium electroplated (400×).

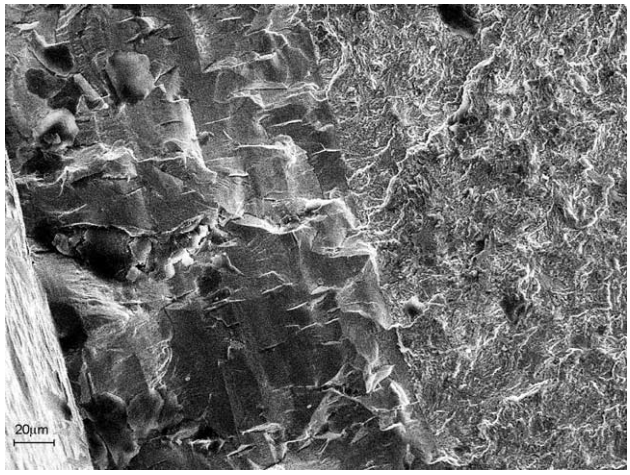

Fig. 5. Fracture surface from specimen hard chromium electroplated (800×).

Table 2
Internal residual stresses

Specimens	Coating surface		Interface coating/substrate		Substrate	
	Residual stress (MPa)	Distance (mm)	Residual stress (MPa)	Distance (mm)	Residual stress (MPa)	Distance (mm)
1	301.9	0.009855	(709.6)	0.0899	(177.4)	0.1950
2	230	0.01016	(457.5)	0.0924	(453.9)	0.1673
3	332.7	0.00889	(687.7)	0.1066	(258.5)	0.1564

HP/HVOF I process. ( ) Represent negative values.

to a stress-relieve heat treatment at 190 °C for 4 h to reduce residual stress induced by machining. Average superficial roughness in the reduced section of the samples was $Ra \approx 2{,}75$ μm and a standard deviation of 0.89 μm.

For axial fatigue tests, a sinusoidal load of 50-Hz frequency and load ratio of R=0.1 was applied throughout this study (I and II). Experimental tests consider as fatigue strength the complete fracture of the specimen or 10^7 load cycles. Eight groups of fatigue specimens were prepared to obtain *S–N* curves for axial fatigue tests.

2.1. Axial fatigue tests

Tungsten carbide thermal spray coated specimens were blasted with aluminum oxide mesh 90 to enhance adhesion. Axial fatigue test specimens were prepared according to standard ASTM E 466 (Table 1).

2.2. Tungsten carbide coating

WC powder with 17% Co (thickness equal to 150 μm). Two high-velocity oxygen-fuel spray systems were responsible for sample preparation.

WC powder with 10% Co and 4% Cr (thickness equal to 170 μm). Two high-velocity oxygen-fuel spray systems were responsible for sample preparation.

2.3. Shot peening

S–N curves were obtained for base metal and shot peening condition of 0.0063 A, carried out on an air-blast machine according to standard MIL-S-13165. Based on scanning electron microscopy coating morphology, microcracks formed in hard chromium plating and fatigue cracks were observed. Analyses of fracture surface were carried out on axial fatigue specimens by scanning electron microscope, model LEO 435 Vpi and Zeiss DSM 950.

2.4. Hard chromium electroplating

The conventional hard chromium electroplating was carried out from a chromic acid solution with 250 g/l of CrO_3 and 2.5 g/l of H_2SO_4, at 50–55 °C, with a current density from 31 to 46 A/dm^2, and a speed of deposition equal to 25 μm/h. A bath with a single catalyst based on sulfate was used. After the coating deposition, samples were subjected to a hydrogen embrittlement-relief treatment at 190 °C for 8 h. Average surface roughness of the hard chromium electroplating was $Ra \approx 3.13$ μm in the reduction section and standard deviation of 0.79 μm in the electroplated condition was observed.

2.5. Salt spray test

The performance of the coating was evaluated with respect to chemical corrosion, in specific environment. Samples were prepared from normalized AISI 4340 steel with 1 mm thickness, and 76 mm width and 254 mm length, surface roughness $Ra \approx 0.2$ μm and in the following conditions:

- WC–10Co–4Cr HP/HVOF I, 100 μm;
- WC–10Co–4Cr HP/HVOF I, 150 μm;
- WC–10Co–4Cr HP/HVOF I, 200 μm;
- WC–17Co HP/HVOF I, 250 μm;
- WC–17Co HP/HVOF I, 250 μm, with sealing.

Experimental tests were conducted in accordance to ASTM B 117, in 5 wt.% NaCl, pH of 6.5–7.2 at 35 °C. Samples were supported at 20° from the vertical. Results were analyzed by Image Pro Plus software.

Table 3
Internal residual stresses

Specimens	Coating surface			Interface coating/substrate			Highest compressive internal residual stress		
	R.S. long. (MPa)	R.S. tras. (MPa)	Distance (mm)	R.S. long. (MPa)	R.S. trans. (MPa)	Distance (mm)	R.S. long. (MPa)	R.S. trans. (MPa)	Distance (mm)
1	449.8	506.5	0.0138	(438.8)	(294.2)	0.2424	(518.9)	(674.3)	0.1935
2	149.6	42.9	0.0147	(124.9)	(272.5)	0.2652	(999.2)	(543)	0.2060
3	113	142	0.0138	(161)	7.7	0.3015	(666.2)	(760.3)	0.2343
4	46.4	116.7	0.0131	(628.6)	(838.4)	0.2781	(628.6)	(838.4)	0.2781

HVOF II process. Coating thickness for specimens tested were 0.2779, 0.2979, 0.3528, and 0.2967 mm, respectively. ( ) Represent negative values.

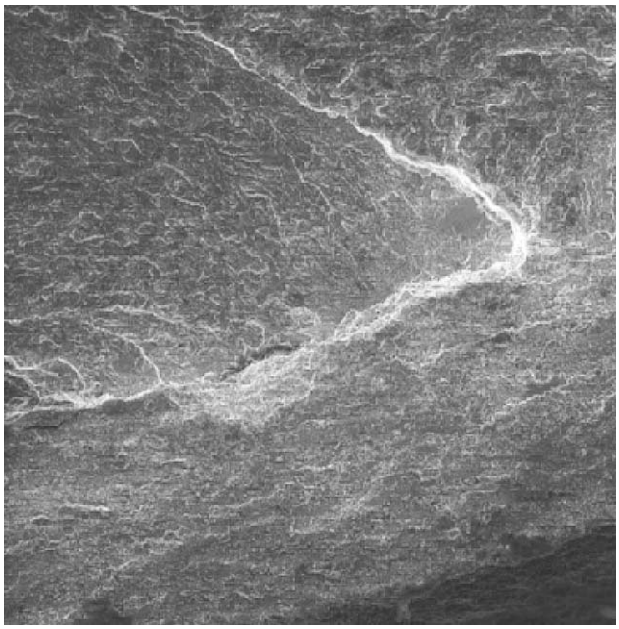

Fig. 6. Fracture surface of axial fatigue specimen coated by HP/HVOF I process and tested at σ=67, 8% of yield strength.

2.6. Abrasive wear test

The performance of the coating was also evaluated with respect to abrasive wear. Samples were prepared from annealed AISI 4340 steel with 4 mm thickness and 100 mm^2, according to FED–STD–141C; and divided in four groups; one coated with 100 μm thickness of hard chromium electroplating, two groups coated with 100 μm thickness of WC–17%Co spray coating by HP/HVOF I spray process and HVOF II spray process, respectively, and one group coated with 100 μm thickness of WC–10Co–4Cr spray coating by HP/HVOF I.

Wear tests were conducted with a Taber Abraser, at room temperature, using a 10-N load and CS-17 abrading wheel for hard chromium electroplating and diamond wheel for tungsten carbide coating. Results were analyzed by wear index (mg/1000 cycles) and total wear (mg/10,000 cycles) data.

Fig. 7. Fracture surface of axial fatigue specimen coated by HP/HVOF II process and tested at σ=67, 8% of yield strength.

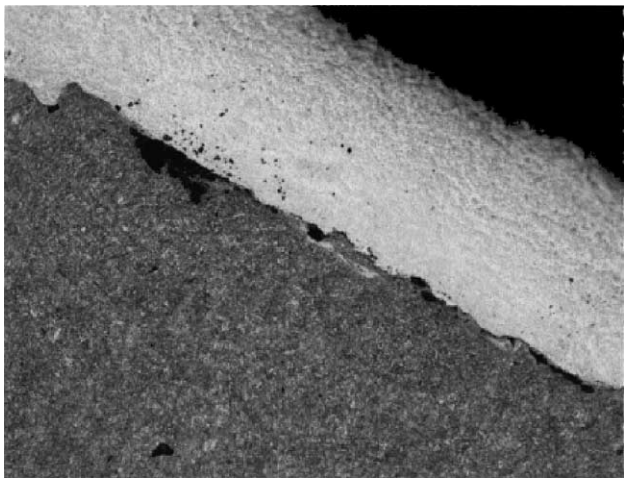

Fig. 8. Coating profile for fatigue specimen coated by HP/HVOF I process.

2.7. Residual stress measurement

The compressive residual stress field induced by shot peening was determined by X-ray diffraction method, using the ray stress equipment, whose characteristics are described in section [29]: ψ goniometer geometer, Cr-Kα radiation and registration of {221} diffraction lines. The accuracy of the stress measurement was $\Delta\sigma=\pm 20$ MPa. In order to obtain the stress distribution by depth, the layers

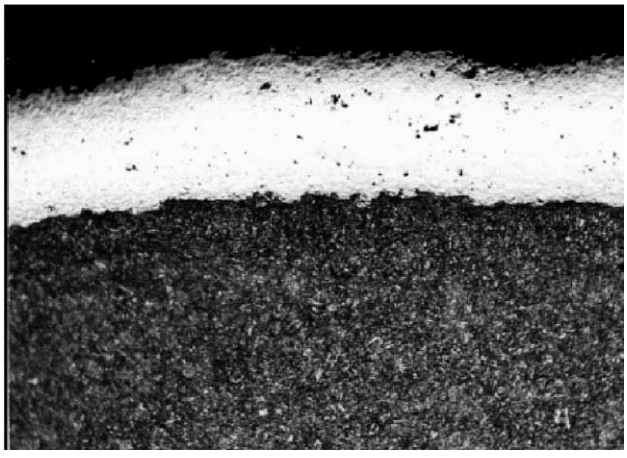

Fig. 9. Coating profile for specimen coated by HP/HVOF II process.

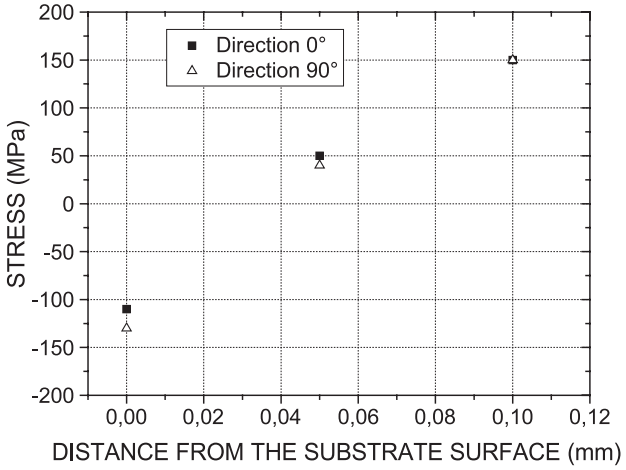

Fig. 10. Through thickness internal residual stress. WC–10Co–4Cr I process.

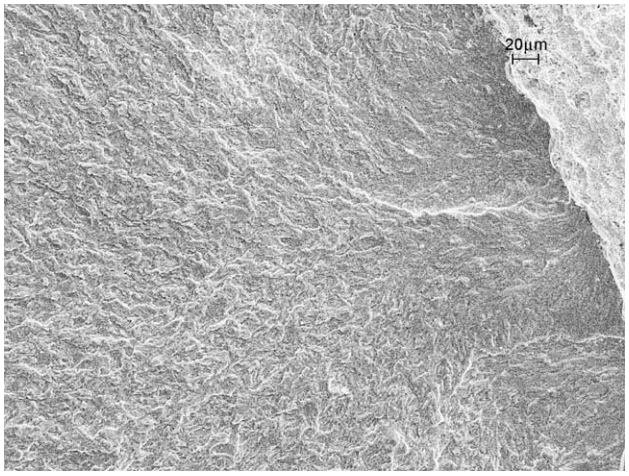

Fig. 12. Fracture surface from specimen shot peened and coated with WC–10Co–4Cr.

of specimens were removed by electrolytic polishing with a nonacid solution.

3. Results and discussion

3.1. Fatigue tests

Fig. 2 shows axial fatigue *S–N* curves for base material, base material electroplated with hard chromium, 160 µm thick, base material with WC–17%Co spray coating by HP/HVOF I process, 150 µm thick, and base material with WC–17%Co spray coating by HVOF II process, 150 µm thick.

Axial fatigue *S–N* curves tests for the base material, base material hard chromium electroplated, 160 µm thick, base material with WC–10Co–4Cr spray coating by HP/HVOF I process 170 µm thick, base material shot peened with WC–10Co–4Cr spray coating by HP/HVOF I process 170 µm thick, base material with WC–10Co–4Cr spray coating by HVOF II process 170 µm thick, and base material shot peened with WC–10Co–4Cr spray coating by HVOF II process 170 µm thick, are presented in Fig. 3a and b, respectively.

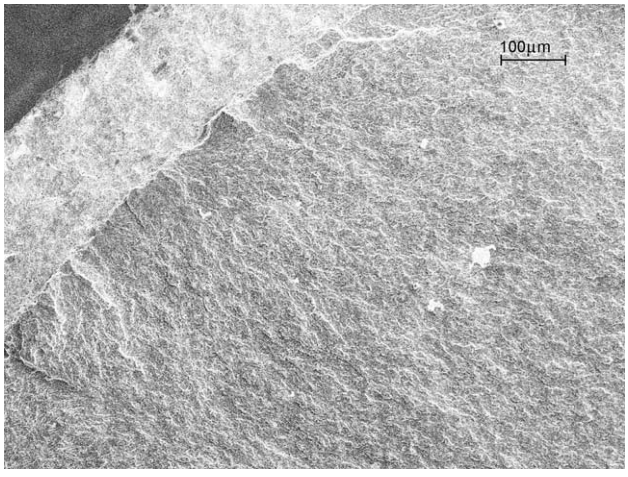

Fig. 11. Fracture surface from specimen coated with WC–10Co–4Cr, 200×.

Analysis of the experimental data indicated in Fig. 2 revealed the significant reduction in the fatigue strength of AISI 4340 steel, associated with the chromium electroplating. This behavior may be attributed to the high tensile internal residual stress, microcracks density and strong adhesion coating/substrate interface. Tungsten carbide thermal spray coating applied by HP/HVOF I process, considered in this research as an alternative to chrome plating, had also a reduction effect on the axial fatigue strength of AISI 4340 steel.

According to the experimental data represented in Fig. 2, the reduction in fatigue life of coated material with WC–17%Co, is more significant in high cycle than in low cycle fatigue tests and the fatigue resistance of the substrate material is less affected by both WC–17%Co spray coated by HP/HVOF I and HVOF II processes, 150 µm thick, respectively, than by hard chromium electroplating, 160 µm thick.

Fracture surfaces analysis from axial fatigue specimens chromium electroplated, indicate in Figs. 4 and 5 coating

Table 4
Abrasive wear weight loss: Hard Chromium plating

Abrasive wear (Taber Abraser)		
Cycles (*N*)	Conventional hard chromium	
	Total (mg)	mg/1000
1000	2.83	2.83
2000	5.57	2.74
3000	8.33	2.76
4000	11.33	3.00
5000	14.83	3.50
6000	17.63	2.80
7000	20.60	2.97
8000	22.93	2.33
9000	25.83	2.90
10 000	29.13	3.30
Average	2.91 mg/1000 cycles	

Table 5
Abrasive wear weight loss: WC–17%Co spray coating by HP/HVOF I process

Abrasive wear (Taber Abraser)		
Cycles (*N*)	WC–17%Co spray coating by HP/HVOF I	
	Total (mg)	mg/1000
1000	1.82	1.82
2000	2.92	1.10
3000	4.22	1.30
4000	5.78	1.56
5000	6.98	1.20
6000	8.24	1.26
7000	9.44	1.20
8000	10.04	0.60
9000	10.60	0.56
10000	10.70	0.10
Average	1.07 mg/1000 cycles	

Table 7
Abrasive wear weight loss: WC–10Co–4Cr spray coating by HP/HVOF I process

Abrasive Wear (Taber Abraser)		
Cycles (*N*)	WC–10Co–4Cr by HP/HVOF I	
	Total (mg)	mg/1000
1000	1.05	1.05
2000	3.55	2.50
3000	4.7	1.15
4000	6.5	1.8
5000	7.1	0.6
6000	8.6	1.5
7000	9.85	1.25
8000	10	0.15
9000	10.1	0.1
10000	11.85	1.75
Average	0.11 mg/1000 cycles	

homogeneity, strong interface substrate/coating and microcracks density distributed along the thickness in a radial shape.

Values of through-thickness residual stresses, obtained by the modified layer-removal method for thermal spray coating and substrates [25,26], show that no significant differences in the residual stresses profile of AISI 4340 steel coated by HP/HVOF I and HVOF II process occur. The through-thickness residual stresses change from tensile, at coating surface to compressive inside coating thickness, with compressive stresses at interface coating/substrate. Inside base metal, stresses change from compressive to tensile at almost the same distance from the interface coating/substrate [30].

Internal residual stresses were obtained from three specimens WC–17%Co spray-coated by HP/HVOF I process and four specimens by HVOF II process. The two high-velocity oxygen-fuel spray systems, which were responsible for sample preparation, induced residual stress in coating and substrate, which varied from tensile at coating surface to compressive inside coating thickness, as indicated in Table 2. High-compressive stresses were identified around interface coating/substrate; inside base metal, residual stresses changed from compressive to tensile increasing distance from interface. Tables 2 and 3 show internal residual stresses results for both systems.

Figs. 6 and 7 show fracture surfaces from axial fatigue specimens coated with HP/HVOF I and HVOF II processes and tested at σ=67, 8% of yield strength, respectively.

For both systems, it is possible to identify the same characteristic of fatigue crack nucleation at the interface coating/substrate. In Fig. 6, fatigue cracks coalescence and propagation inside substrate is preceded by crack growth at interface. Despite the compressive internal residual stresses inside the coating and at coating/substrate interface induced by HVOF processes, experimental results show reduction in the axial fatigue strength of coated AISI 4340 steel in comparison to base metal.

Figs. 8 and 9 represent coating profiles for HP/HVOF I and HVOF II processes, respectively.

The decrease in fatigue strength induced by the HVOF processes may be associated to the high density of porous and oxide inclusions into the coating, which are possible crack nucleation/initiation sites. From Figs. 8 and 9, it is possible to observe coating homogeneity, strong interface substrate/coating, increase in roughness at interface coating/

Table 6
Abrasive wear weight loss: WC–17%Co spray coating by HVOF II process

Abrasive wear (Taber Abraser)		
Cycles (*N*)	WC–17%Co by HVOF II	
	Total (mg)	mg/1000
1000	0.93	0.93
2000	1.21	0.28
3000	1.52	0.31
4000	2.18	0.66
5000	2.61	0.43
6000	2.87	0.26
7000	2.97	0.10
8000	3.03	0.06
9000	3.09	0.06
10000	3.12	0.03
Average	0.31 mg/1000 cycles	

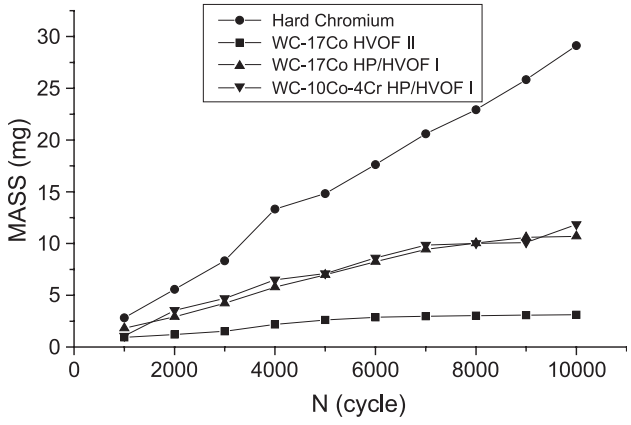

Fig. 13. Abrasive wear weight loss versus number of cycle.

Table 8
Through thickness HV microhardness with 1 N load for hard chromium electroplating

Hard chromium	
Surface distance (mm)	Microhardness (HV)
0.05	897
0.10	906
0.15	912
Interface	–

Table 10
Through thickness HV microhardness with 1 N load for WC–17%Co HVOF II

WC–17%Co HVOF II	
Surface distance (mm)	Microhardness (HV)
0.05	1225
0.10	1097
0.15	1287
Interface	–

substrate due to aluminum oxide blasting, increasing adhesion and that, in both cases, the deposition process did not affect the microstructure.

Axial fatigue *S–N* curves for the base material, base material electroplated with hard chromium, base material with WC–10Co–4Cr spray coating by HP/HVOF I process, base material with WC–10Co–4Cr spray coating by HVOF II process, base material shot peened with WC–10Co–4Cr spray coating by HP/HVOF I process, and base material shot peened with WC–10Co–4Cr spray coating by HVOF II process, are present in Fig. 3a and b.

These figures show that the effect of coating is to decrease the axial fatigue strength of AISI 4340 steel. Similar to the experimental results from Fig. 2, it is possible to observe a significant reduction in the fatigue strength associated to chromium electroplating, in comparison to specimens coated with WC–10Co–4Cr applied by HP/HVOF I and HVOF II processes. This lower decrease in fatigue strength may be attributed to the process itself because it is well known that HVOF thermal spray produces compressive internal residual stresses within the substrate [30], which are formed from mechanical deformation on surface caused by particle impact of coating in the substrate.

Fig. 10 shows internal residual stresses in the substrate for specimens coated with WC–10Co–4Cr applied by HP/HVOF I process.

Experimental results in Fig. 10 indicate, in the same way as data from Table 2, compressive internal residual stresses at coating/substrate interface, increasing into the base metal becoming tensile at around 0.03 mm from the interface.

The reduction in the fatigue strength of AISI 4340 steel coated with WC–10Co–4Cr, despite the compressive internal residual stresses induced by both processes studied, may be justified in the same way for WC–17%Co; high density of porous and oxide inclusions into the coating that commonly forms during the process.

Thermal spray is generally conducted in air, so chemical interactions occur, notably oxidation, which can be evident in the coating microstructure as oxide inclusions, mainly in grain boundaries. These inclusions in coating/subsurface are possible cracks nucleation/initiation sites. Fig. 3a and b show that the decrease in fatigue strength of specimens coated with WC–10Co–4Cr applied by HP/HVOF I and HVOF II processes was totally recovered by the shot peening process. It is well known that fatigue crack initiation occurs at surface [19], depends on the residual stress profile on it and that compressive residual stress delay fatigue crack propagation.

In previous work [19], it was observed that despite the fact that an increase in shot peening intensity resulted in an increase in the maximum compressive residual stress and width of the compressive residual stress field; the surface residual stress was nearly independent of the peening conditions. The shot peening process pushes the crack sources beneath the surface in most of medium and high cycle cases due to the compressive residual stress field induced. Fig. 11 shows a fracture surface from an axial fatigue specimen coated with WC–10Co–4Cr applied by HP/HVOF I process, 170 μm thick and tested at 71% of the yield strength. It is possible to observe cracks starting at the interface coating/substrate.

Analysis of Fig. 12, that represents a fracture surface from an axial fatigue specimen shot peened and coated with WC–10Co–4Cr applied by HP/HVOF I process, 170 μm thick and tested at 89% of the yield strength, indicate fatigue crack nucleation and propagation from interface coating/substrate throughout base metal. In the same figure, cracks sourced below the coating/substrate interface induced by shot peening treatment are correlated to gain in fatigue life.

In Figs. 11 and 12, fatigue source appearance is distributed around specimen surface as a consequence of

Table 9
Through thickness HV microhardness with 1 N load for WC–17%Co HP/HVOF I coating

WC–17%Co HP/HVOF I	
Surface distance (mm)	Microhardness (HV)
0.05	1032
0.10	1168
0.15	1249
Interface	–

Table 11
Through thickness HV microhardness with 1 N load for WC–10Co–4Cr HP/HVOF I coating

WC–10Co–4Cr HP/HVOF I	
Surface distance (mm)	Microhardness (HV)
0.05	1120
0.10	1047
0.15	1187
Interface	–

Table 12
Through thickness HV microhardness with 1 N load for WC–10Co–4Cr HVOF II coating

WC–10Co–4Cr HVOF II	
Surface distance (mm)	Microhardness (HV)
0.05	1174
0.10	1167
0.15	1040
Interface	–

the influence of coating on fatigue crack nucleation. In the same figures, WC–10Co–4Cr applied by HP/HVOF I and HVOF II processes resulted in coating homogeneity, strong coating/substrate interface, and increase in roughness at coating/substrate interface.

3.2. Abrasive wear test

The abrasive wear resistance of hard chromium plating, WC–17%Co spray coating by HP/HVOF I and II processes and WC–10Co–4Cr spray coating by HP/HVOF I process were evaluated and results in terms of wear weight loss are represented in Tables 4–7 and in Fig. 13.

One sees the better performance of samples coated with WC, with lower-wear weight loss than the hard chromium-electroplated specimens. This behavior may be attributed to the higher hardness and oxide content into the tungsten carbide coating [16].

Tables 8–12 indicate microhardness for samples chromium electroplated; WC–17%Co HP/HVOF I/HVOF II and WC–10Co–4Cr HP/HVOF I/HVOF II processes coated, respectively.

Fig. 14. Salt spray tests results for WC–17%Co HVOF I, 250 μm thickness.

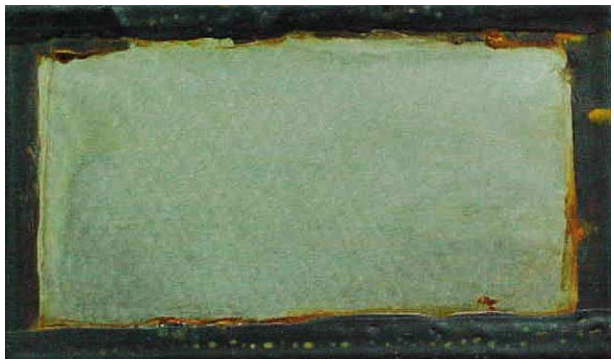

Fig. 15. Salt spray tests results for WC–10Co–4Cr, 100 μm thickness.

Higher microhardness values for WC–17Co spray coating by HVOF II in comparison to HP/HVOF I and hard chromium electroplating explain the results shown in Fig. 13. The wear weight loss for hard chromium electroplating is also associated to the microcrack density. Coating of high oxide content is usually harder [16] and is more wear-resistant [12]. Initially, in the first 1000 cycles, an almost equivalent value of wear weight loss was observed for tensile carbide coatings and hard chromium electroplating. A compensation effect between microhardness and higher-surface roughness of the tungsten carbide coatings, in comparison to the electroplate hard chromium, was responsible for this behavior.

3.3. Salt spray tests

Results of corrosion testing performed in a qualitative way were obtained by visual inspection of the specimen surface exposed to salt spray. For the WC–17%Co HP/HVOF I specimen, 250 μm in thickness, the coating did not quite protect the substrate against the aggressive action of salt spray environment, as indicated in Fig. 14, which shows corrosion products on the sample surface. The same behavior was observed for thickness equal to 150 and 200 μm.

For the HP/HVOF I tungsten carbide coating, Fig. 15 shows that better corrosion resistance was obtained after sealing application before testing, for thickness equal to 100 μm.

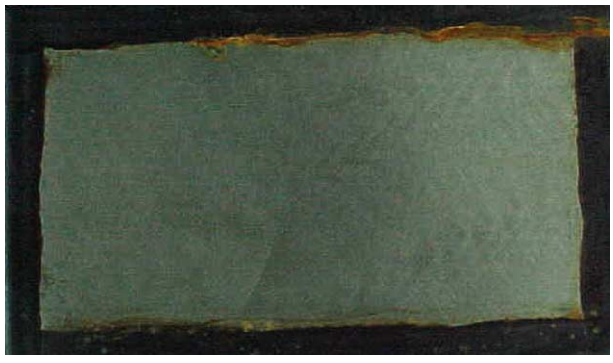

Fig. 16. Salt spray tests results for WC–10Co–4Cr, 150 μm thickness.

Fig. 17. Salt spray tests results for WC–10Co–4Cr, 200 μm thickness.

The salt spray test results for samples WC–10Co–4Cr coated, applied by HP/HVOF I process are shown in Figs. 16 and 17, for thicknesses equal to 150 and 200 μm, respectively.

The surface aspect after salt spray testing indicated no visual corrosion and was observed on samples WC–10Co–4Cr coated.

Hard chromium electroplating process yielded deep microcracks. It is also well known that the increase in thickness enhance the hard chromium protection to the salt spray corrosion [9]. This corrosion is due to high content of porous and microcracks that lead the corrosive process to the coating/substrate interface.

4. Conclusions

- Experimental results indicate a significant reduction in the fatigue strength of AISI 4340 steel associated with chromium electroplating.
- For axial fatigue tests, fatigue life of AISI 4340 steel is less affected by both WC–17%Co spray-coated by HP/HVOF I and HVOF II processes 150 um thick than by hard chromium electroplating 160 um thick. No significant difference in fatigue strength of AISI 4340 steel coated by HP/HVOF I and HVOF II processes was observed.
- The two high-velocity oxygen-fuel spray systems, which were used for sample preparation, induced residual stresses in coating and substrate, which changed from tensile near the coating surface to compressive inside the coating thickness. High compressive stresses were identified around the interface coating/substrate; inside base metal, residual stresses changed from compressive to tensile with increasing distance from the interface.
- The base material shot peened and coated with WC–10Co–4Cr applied by HP/HVOF I process and HVOF II process recovered totally the decrease in fatigue strength probably due to the superposition the compressive residual internal stresses induced by HVOF thermal spray and shot peening processes.
- With respect to abrasive wear resistance, better performance of samples coated with WC and lower wear weight loss than hard chromium electroplated specimens was observed. This behavior may be associated with the higher hardness and oxide content into the tungsten carbide coating.
- In salt spray test results no visual corrosion was observed on samples WC–10Co–4Cr coated.

Acknowledgements

The support provided by FAPESP through the processes number 98/02186-2 and 97/01160-7, is acknowledged.

References

[1] B.E. Bodger, R.T.R. Mcgrann, D.A. Somerville, Plating Surf. Finish. (1997 (Sept.)) 28.
[2] J.M. Tyler, Metal Finishing (1995) 11.
[3] E. Broszeit, C. Friedrich, G. Berg, Surf. Coat. Technol. 115 (1999) 9.
[4] P.M. Natishan, S.H. Lawrence, R.L. Foster, J. Lewis, B.D. Sartwell, Surf. Coat. Technol. 130 (2000) 218.
[5] A.R. Jones, Plating Surf. Finish. (1989 (April)) 62.
[6] G. Dulpernell, F.A. Lowenheim, Modern Electroplating (1968) 80.
[7] H. Kuo, J. Lai, T. Lin, Int. Arch. Occup. Environ. Health 70 (1997) 272.
[8] K.L. Lin, C.J. Hsu, J.T. Chang, J. Mater. Eng. Perform. 1 (3) (1992 (June)) 359.
[9] M.P. Nascimento, H.J.C. Voorwald, R.C. Souza, W.L. Pigatin, Plating Surf. Finish. 80 (2001) 84.
[10] R.M. Pelloux, Case studies of fatigue failures in aeronautical structures, Proceedings of Conference Fatigue 93. Montreal, 1993, p. 1727.
[11] M.P. Peres, H.J.C. Voorwald, Effect of cadmium deposition on fatigue strength of 4340 steel, Proceedings of fatigue 96, p. 1421.
[12] M.P. Nascimento, R.C. Souza, I.M. Miguel, W.L. Pigatin, H.J.C. Voorwald, Surf. Coat. Technol. 138 (2001) 113.
[13] U. Wicklund, P. Hedernqrist, S. Hogmark, Surf. Coat. Technol. 97 (1997) 773.
[14] R.C. Souza, M.P. Nascimento, H.J.C. Voorwald, W.L. Pigatin, J. Mech. Behav. Mater. 12 (3) (2001) 121.
[15] J. Pina, A. Dias, M. François, J.L. Lebrun, Surf. Coat. Technol. 96 (1997) 148.
[16] M.P. Nascimento, R.C. Souza, W.L. Pigatin, H.J.C. Voorwald, Int. J. Fatigue 23 (2001) 607.
[17] E.R. De los Rios, A. Walley, M.T. Milan, G. Hmmersley, Int. J. Fatigue 17 (7) (1995) 493.
[18] C.P. Diepart, Mat. Sci. Forum 163–165 (1994) 457.
[19] M.A.S. Torres, H.J.C. Voorwald, Int. J. Fatigue 24 (2002) 877.
[20] K. Schiffner, C.D. Helling, Compos. Struct. 72 (1999) 329.
[21] J.K. Li, R. Zhang, M. Yao, ICRS 3 (1991) 1284.
[22] A.T. Özedemir, L. Edwards, Fatigue Fract. Eng. Mater. Struct. 20 (10) (1997) 1443.
[23] H. Holzapfel, Mater. Sci. Eng., A. Struct. Mater.: Prop. Microstruct. Process. 248 (1998) 9.
[24] O. Vöhringer, Adv. Surf. Treat. (1987) 367.
[25] L. Pejryd, J. Wigren, D.J. Greving, J.R. Shadley, E.F. Rybicki, J. Therm. Spray Technol. 4 (3) (1995 (Sept.)) 268.
[26] D.J. Greving, J.R. Shadley, E.F. Rybicki, J. Therm. Spray Technol. 3 (4) (1994 (Dec.)) 371.
[27] M.P. Nascimento, H.J.C. Voorwald, W.L. Pigatin, R.C. Souza, Proceedings of EBRATS 2000, São Paulo, Brazil, may, CD-ROM2000.
[28] J.M. Guilemany, J.M. Paco, Surf. Eng. 14 (2) (1998) 129.
[29] T. Gurova, J.R. Teodósio, J.M.A. Rebello, V. Monin, Scr. Mater. 36 (9) (1997) 1031.
[30] R.C. Souza, M.P. Nascimento, H.J.C. Voorwald, W.L. Pigatin, Corros. Rev. 21 (1) (2003) 75.